A NEW PERSPECTIVE ON THE VERTICAL DISTRIBUTION OF DUST IN THE MARTIAN ATMOSPHERE DURING NORTHERN SUMMER FROM MARS CLIMATE SOUNDER: ELEVATED MAXIMA IN DENSITY-SCALED OPACITY OVER THE TROPICS.

N. G. Heavens[1] and M. I. Richardson[1], D.J. McCleese[2] and the MCS Science Team [1]Division of the Geological and Planetary Sciences, California Institute of Technology, MC 150-21, 1200 E. California Blvd., Pasadena, CA, 91125 (Corresponding author's e-mail: heavens@gps.caltech.edu) [2]Jet Propulsion Laboratory, California Institute of Technology, Pasadena, CA, 91109

Introduction: Because it is strongly radiatively active and highly temporally and spatially variable in its abundance, suspended dust is the martian atmosphere's most meteorologically important component. Vertical profiles of temperature, pressure, dust, and other aerosol retrieved from Mars Climate Sounder (MCS) observations are now providing an expansive dataset that can describe much of this variability [1, 2].

Information about the vertical distribution of dust can provide insights into the mechanisms by which dust enters and leaves the atmosphere. B.J. Conrath [3], for instance, reduced the vertical distribution to the competing effects of sedimentation and vertically uniform vertical eddy diffusion. This simple picture has been complicated by: (1) the possibility of additional removal processes such as the enhancement of sedimentation by the condensation of volatiles on dust particles [4] (2) more detailed modeling of vertical transport above the boundary layer as driven by a combination of dynamical processes such as the thermal tides [5]; (3) more detailed treatment of mixing within the boundary layer [6]; (4) explicit accounting for multiple dust sizes [7]; and (5) consideration of particular dust sources such as mountain slopes [8, 9] and dry convective helical vortices ("dust devils") [10, 11, 12]. These processes have been investigated primarily by modeling and observation of surface features. Observational constraints on these processes would be helpful.

Using zonally-averaged MCS profiles of dust opacity, *Heavens et al.* (this meeting) observed a persistent maximum in density-scaled opacity centered at ~15 km altitude in the tropics, which for shorthand, will be called "the pulse." Note that for dust of uniform (or sufficiently similar) size, shape, and composition, density-scaled opacity is linearly proportional to dust mass mixing ratio. This observation suggests some intriguing questions, e.g., (1) Is the pulse as zonally homogenous and temporally persistent as it appears from zonally-averaged profiles?; (2) what is the pulse's origin?; (3) How are radiative effects of the pulse important for the large-scale circulation?

Possible Origins of the Pulse: Four explanations for the pulse occur within the limited imagination of the corresponding author: (1) exceptionally dust-laden plumes as in dust devils or "dust cells" often seen at the leading edge of dust storms [13] gain positive buoyancy through absorption of solar radiation and rise with minimal detrainment above the well-mixed boundary layer, where they detrain as solar heating decrease and mix on local scales [14]; (2) dust is lifted by topographically-forced mesoscale circulations along slopes and injected at height [9]; (3) dust, especially smaller particles, is primarily raised near the surface in a region other than those underlying the pulse and then transported by the Hadley cell or similar circulation into the tropics aloft, enhancing mass mixing ratios there relative to the boundary layer [7]; or (4) enhanced sedimentation of condensate-coated dust within water ice clouds results in a slowly settling layer of enhanced dust below the cloud once the ice sublimes.

Methods: At present, atmospheric retrievals from Mars Climate Sounder observations (see *Kleinböhl et al.*, this meeting) provide vertical profiles of pressure (Pa), temperature (K), dust opacity, i.e., fractional extinction due to dust per unit height ($d_z\tau$), (km^{-1}) at 463 cm^{-1}, and water ice opacity (km^{-1}) at 842 cm^{-1}. The approximate ratio between the dust opacity at 463 cm^{-1} and visible dust opacity at 660 nm can be modeled to be ~4.3, and this ratio will be adopted for the purposes of this paper.

The retrievals are from a preliminary version of the standard Level 2 limb retrieval product delivered to the Planetary Data System, primarily differing in gridding, extrapolation, and post-processing as opposed to the retrieval algorithm. And thus the results of this study should be nearly reproducible from the standard product and the fitting scheme used in the study likewise applicable. One key element of this retrieval dataset is that information about dust from the detector observing the limb at ~8 km above the surface (detector 19 of channel A5) is used. The retrieval algorithm and post-processing also may bias sampling away from profiles over topography or those that are especially dusty and icy. The key extrapolations are constant dust mass mixing assumptions at the top and the bottom of the profile. The former extrapolation is not necessary for the fitting scheme, but the latter is essential.

34505 retrievals are available that satisfy these criteria and are available for the period during L_s=111°-168°. The dust opacity retrievals were fit by a scheme that represents density-scaled opacity as a function of σ **(**for these purposes defined as the ratio between the pressure and the surface pressure**).** This scheme assumes a constant value at the bottom of the profile. The decay with decreasing σ is fit with a gaussian truncated using a Heaviside function. Up to two peaks in density-scaled opacity are fit with gaussians as well. Fisher ratio tests are used to minimize overfitting. In addition, the scheme diagnoses where the constant mass mixing ratio extrapolation occurs at the top of the profile and does not fit the extrapolated values. The temperature and pressure retrievals also are used to estimate a near-surface air density and scale height over 5-20 km.

The scheme fails for two pathological cases: (1) extremely clear profiles where dust is effectively not retrieved; (2) profiles where a peak is not resolved because a detector is "thrown out" at the top of the retrieval. In both of these cases, the scheme may fit very poorly (in terms of explanation of variance) or assume dust mixes to "infinite height" in the atmosphere. Thus, the retrievals used here must fulfill two conditions: the scheme explains 90% of the variance and the extrapolated dust opacity at the surface is $2.78*10^{-5}$ km^{-1}. These conditions eliminate most, but not all of the pathological retrievals, reducing the number of retrievals used to 25669.

Once fit, various convenient quantities can be calculated such as I (the near-surface density scaled opacity), P_1, (the density-scaled opacity due to the largest pulse in the profile), P_2 (the the density-scaled opacity due to the second largest pulse in the profile), and Z_{p1} (the height above the local surface of the largest peak in the pulse) etc. For reference, the conversion between density-scaled opacity in m^2 kg^{-1} to ppbm (parts per billion by mass) is $1.1*10^4$ assuming spherical particles of 1.47 μm radius and Q_{ext}=0.5351 at 463 cm^{-1}.

Results:

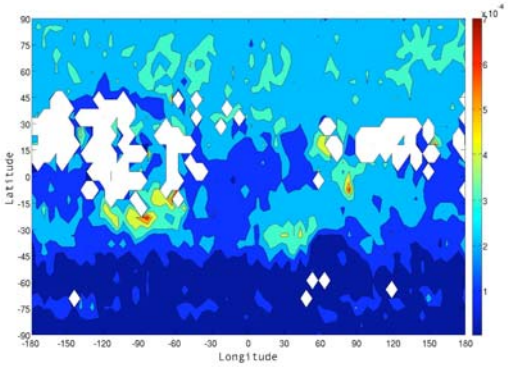

Figure 1: I (m^2 kg^{-1}) averaged in 5°x5° bins over L_s=111°-168°

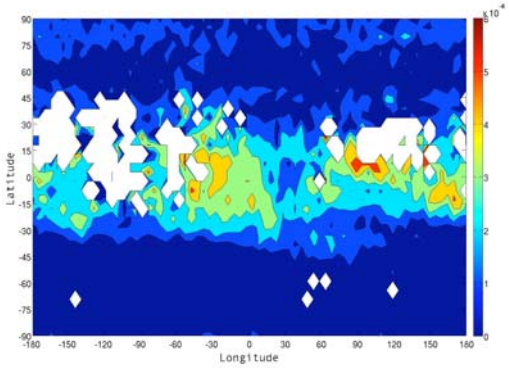

Figure 2: P_1 (m^2 kg^{-1}) averaged in 5°x5° bins over L_s=111°-168°

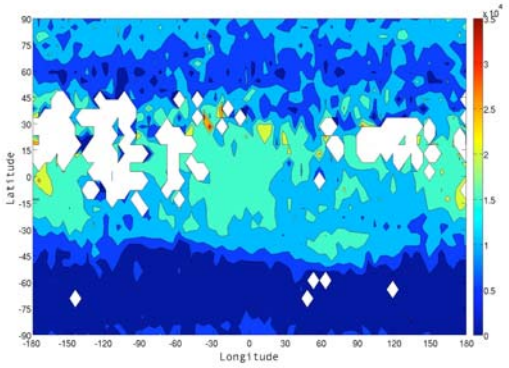

Figure 3: Z_{p1} (m) averaged in 5°x5° bins over L_s=111°-168°

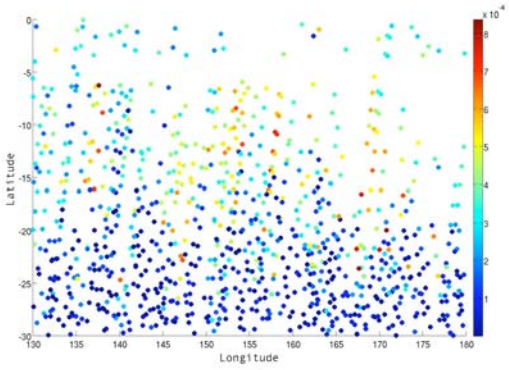

Figure 4: Scatter plot of P_1 (m^2 kg^{-1}) for individual retrievals within 130°-180° E, 30°-0° S over L_s=111°-168°.

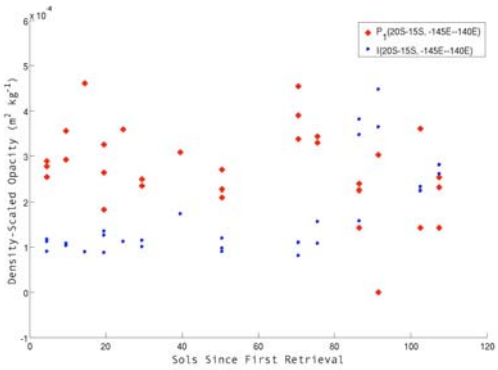

Figure 5: P_1 (m^2 kg^{-1}) for a tropical 5ºx5º box (20º-15º S, -145º— -140º E) over L_s=111º-168º chosen for its frequent sampling (time scale is in sols for clarity)

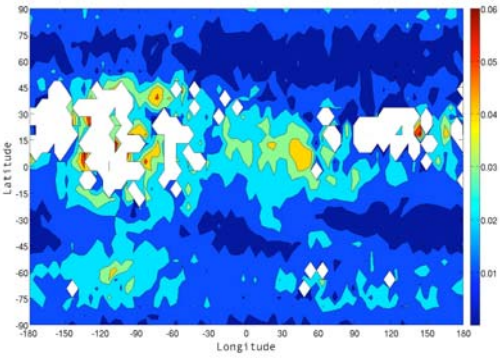

Figure 6: $\tau_{water\ ice}$ averaged in 5°x5° bins over L_s=111°-168°

Discussion: Figure 1 shows the mean value of *I* over the period, showing the generally greater dustiness of the northern hemisphere relative to the south in this period. Unusually high lower level dustiness is evident in Syria and Sinai Plana, northern Noachis Terra, the Syrtis-Isidis boundary, and south of the Elysium Montes. The first region is well-known in this period for its "dust cell" activity after L_s=~135° [13] and there appears to be a definite increase in *I* after ~ L_s=140 here. Northern Noachis appears to be merely the most intense part of the "southern source" activated after L_s=140 mentioned by *Heavens et al.* (this meeting). Observations in earlier years suggest that local dust storm activity at ~45°S does increase during this period [13, 15]. The latter two areas are places in which contrasts in either topography or albedo/thermal inertia contrasts may result in frequent intense mesoscale circulations capable of dust lifting, though local dust storm activity is not particularly concentrated there during this period [15]. The general pattern of *I* in the tropics appears coincident with topography (as opposed to albedo). *I* is relatively low over lower elevation Chryse-Margaritifer-Meridiani, but higher over Syrtis-Tyrrhenum-Hesperia. This may reflect biasing of *I* over areas with shallow boundary layers by extrapolation of constant mass mixing ratio to the surface. Recent results suggest lower topography areas tend to have shallower boundary layers [16].

Figure 2 shows the mean value of P_1 for the period. In some cases, P_1 and *I* appear anti-correlated. P_1 is typically high over the lower topography Chryse-Margaritifer-Meridiani region. But is also high along the albedo-topography boundary on the northern edge of Terra Tyrrhenum and Hesperia Planum, where *I* values are typical for the tropics. This latter region, too, might be a good place for mesoscale circulations, though there is little indication it is particularly prone to dust storm activity [15].

Figure 3 shows the mean value of Z_{p1} for the period and suggests that the peak pulse (in the regions where it is most intense) is generally >15 km above the surface, though slightly lower on the northern edge of Hesperia Planum.

Focusing on this region in Figure 4, P_1 as derived from individual retrievals is plotted. Substantial variability in small areas is observed, suggesting temporal variability in the pulse over the ~100 sols sampled. But how much variability can be expected?

The pulse observed in any given small area (~ 300x300 km or ~5°x5°) should have a few characteristic time periods associated with it. First, there is the time period of sedimentation. A particle with a radius of 1.5 μm will have a fall velocity of ~$5*10^{-3}$ ms^{-2} as a sphere and around half that as a disk [17] at 10 km and a slightly greater fall speed at 15 km. The major source of vertical diffusivity at that height will be due to the large-scale Hadley circulation, which will have some impact on the dissipation of the pulse in the horizontal. But neglecting vertical diffusivity, the sedimentation timescale of the pulse should be 10-20 sols. Horizontal winds at 10-15 km in the tropics are relatively weak, O(1 ms^{-1}), which implies that horizontal dissipation of the pulse to the background mean should take ~5 sols. The final important timescale (which is unknown to us) is the timescale of the source.

In Figure 5, we focus on a 5°x5° region in the tropics with the highest number of retrievals, plotting *I* and P_1. There are two issues with deciphering this plot. First, the approximate sampling frequency of this region is once per five days. Second, the variability in P_1 (and likely *I* as well) over the region within a single orbit (a few minutes in time) is fairly significant relative to variability between times. Some of this may be artifacts of the retrieval and processing. Averaging over an individual orbit does produce less noisy re-

sults, but it also implies some sort of variability on the timescale of sampling, possibly having to do with dissipation by horizontal advection/diffusion.

What Figure 5 does show is an increase in I around sol 90 (L_s=156°) and a reduction in P_1, possibly suggesting an increase in dust storm activity and more direct vertical mixing between the boundary layer and 10-20 km, which in effect mixes out the pulse, so that it is either not resolved (P_1=0) or less well-resolved.

These analyses do not provide as much insight into the pulse's origins as hoped (though they do suggest substantial spatial inhomogenity and some temporal variability), in part because it is difficult to match these spatial inhomogeneities to the optical observational records of dust storms and dust devils. Since local dust storms are larger (and thus easier to see), it is likely that dust storm activity near the equator during this period is limited to the vicinity of Valles Marineris [15]. However, estimates of dust devil activity based on dust devil track coverage [18] and from observations of dust devils at the same local time [11] disagree about the levels and locations of equatorial dust devil activity (the track method suggests equatorial activity is present but infrequent in comparison with ~60° N and S). In small areas where dust devil activity is exceptional (NW Amazonis Planitia), retrievals are few (though the pulse is present in some of them).

What is clearer is that the pulse probably is not the result of a synoptic or global-scale transport process. While the northern hemisphere is slightly more dusty than the southern hemisphere, it is not exceptionally so and it seems unlikely that dust rising in the winter Hadley cell displaced north of the equator is enhancing dust mass mixing ratios over the tropics. Indeed, such a process would result in a pulse that looked very much like the source longitudinally, which is not observed. Such a source also would be required to produce a enhanced sedimentation below water ice clouds.

Some kinds of topographically-forced circulations look to be improbable dust sources as well. Mars' equatorial easterlies could advect dust at 15-20 km from the Tharsis Montes into the eastern hemisphere, but explaining the pulse maximum further downwind would require a mountain range of similar size in eastern Arabia Terra. However, some sort of mesoscale topographic circulation could be one possible driving mechanism behind the pulse source.

Having dismissed these sources, (mainly on hearsay) is it physically plausible for dust devils or dust plumes of similar particle densities (perhaps created by strong winds blowing downslope as in some terrestrial haboobs) to be the pulse source? The estimated mass mixing ratio of a dust devil is ~4500 ppbm [13]. The density of a pulse with P_1=5*10^{-4} m^2 kg^{-1} is 5.5 ppbm. If the dissipation time is ~5 sols, dust devils only occur for an hour per day (allowing only two plumes occupying similar areas to lift dust to sufficient height at 10 ms^{-1} vertical velocity), the necessary areal fraction covered by sufficiently intense dust devils during the active period each day is 1.2*10^{-4}. This areal fraction is about 5-10x lower than the areal fraction of large dust devils observed in the densest activity, assuming a dust devil area of ~0.5 km^2 [11]. Moreover, the heights of dust devils in such activity can be up to 8.5 km high (as inferred from optical imagery) [19]. Note, however, that a dust devil source for the pulse would imply much higher densities of dust devil activity in the tropics at some time of day not covered by current optical observations.

In terms of radiative forcing in the context of large-scale dynamics, the pulse is interesting in that it does seem to co-exist with thin water ice clouds rather than being below water ice clouds. Note, though, that retrievals in areas with high amounts of water ice (as implied by Figure 6) are quite limited. During the daytime, planetary wave activity could be stimulated by contrast between heating of the pulse at rates of 4-20 K sol^{-1} (higher if scattered radiation is more efficiently re-absorbed than 10%) and cooler areas beneath higher amounts of water ice cloud. The effects of equatorial water ice on the large-scale dynamics recently has been considered [20] and appears significant to the entirety of the global circulation. The effects of pulse dust (as well as its source) requires future consideration in modeling.

References: [1] D.J. McCleese *et al.* (2007), *JGR*, **112**, E05S06; [2] D.J. McCleese *et al.* (2008), *Nature Geosci.*, in press; [3] B.J. Conrath (1975), *Icarus*, **24**, 36-46; [4] S.M. Nelli and J.R. Murphy (2003), 200th AAS Meeting, 12.02; [5] R.J. Wilson and K. Hamilton (1996), *JAS*, **54**, 1290-1326; [6] P.A. Taylor *et al.* (2007), *Bound. Lay. Met.*, **125**(2), 305-328; [7] M.A. Kahre *et al.* (2008), *Icarus*, **195**, 576-597; [8] S.W. Lee *et al.* (1982), *JGR*, **87**, 10025-10041; [9] S.C.R. Rafkin *et al.* (2002), *Nature*, **419**, 697-699; [10] M.A. Kahre *et al.* (2006), *JGR*, **111**, E06008; [11] B.A. Cantor *et al.* (2006), *JGR*, **111**, E12002; [12] R. Greeley *et al.* (2006), *JGR*, **111**, E12S09; [13] B. Cantor *et al.* (2002), *JGR*, **107** (E3), 3.1-3.8. [14] S.D. Fuerstenau (2006), *GRL*, **33**, L19S03; [15] B.A. Cantor *et al.* (2001), *JGR*, **106** (E10), 23653-23687; [16] D.P. Hinson *et al.* (2008), *Icarus*, in press, doi:10.1016/j.icarus/2008.07.003; [17] J.R. Murphy *et al.* (1990), *JGR*, **95**, 14629-14648; [18] P.L. Whelley and R. Greeley (2008), *JGR*, **113,** E7002; [19] J.A. Fisher *et al.* (2005), *JGR*, **110**, E3004; [20] R.J. Wilson *et al.* (2008), *GRL*, **35**, L07202.